Aging effect and large recoverable electrostrain in Mn-doped $KNbO_3$-based ferroelectrics

Zuyong Feng and Xiaobing Ren[a)]
Ferroic Physics Group, National Institute of Materials Science, Tsukuba, Ibaraki 305-0047, Japan

(Received 10 May 2007; accepted 17 June 2007)

$KNbO_3$-based ferroelectrics have drawn much attention in recent years owing to their good piezoelectric performance among Pb-free piezoelectrics. However, little is known about the aging effect of these materials. In the present study, the authors systematically studied the aging effect of a Mn-doped $(K_{0.99}Li_{0.01})(Nb_{0.65}Ta_{0.35})O_3$ ceramic with an aim to find an aging-induced recoverable electrostrain effect based on a reversible domain switching mechanism. They found that aging in the ferroelectric state made the otherwise normal hysteresis loop into a double loop, and more interestingly the aged sample demonstrated a large recoverable electrostrain of 0.125% at 4 kV/mm in an unpoled state. Such a behavior persisted up to 140 °C and showed good recoverability. The aging-induced double hysteresis and recoverable electrostrain suggest a reversible domain switching mechanism due to a symmetry-conforming short-range ordering of point defects. The striking similarity of the aging effect between acceptor-doped $A^{+}B^{5+}O_3$ and acceptor-doped $A^{2+}B^{4+}O_3$ systems indicates a common physical origin of aging. *© 2007 American Institute of Physics*.
[DOI: 10.1063/1.2756355]

Because of the urgent demand for Pb-free piezoelectrics, $KNbO_3$-based $A^{+}B^{5+}O_3$ ferroelectrics with perovskite structure are drawing considerable interest for their good piezoelectric properties with high Curie temperature.[1–6] However, in this class of ferroelectrics little is known about the aging effect, which is a spontaneous change of ferroelectric, dielectric, and piezoelectric properties with time. The aging effect has been commonly observed in acceptor-doped $A^{2+}B^{4+}O_3$ ferroelectric perovskites such as $Pb(Ti,Zr)O_3$ and $BaTiO_3$ systems,[7–10] Recently, it has been used to generate a large *recoverable* nonlinear electrostrain in acceptor-doped $BaTiO_3$ single crystals and ceramics.[11–14]

In this letter we report the aging effect and the associated large electrostrain effect in an acceptor-doped $A^{+}B^{5+}O_3$ ferroelectric system: Mn-doped $KNbO_3$-based piezoceramic $(K_{0.99}Li_{0.01})[(Nb_{0.65}Ta_{0.35})_{0.99}Mn_{0.01}]O_3$. As will be seen in the following, after aging, we found an interesting *double*-hysteresis loop and large recoverable electrostrain behavior in this acceptor-doped $A^{+}B^{5+}O_3$ ferroelectrics, being strikingly similar to the aging effect in acceptor-doped $A^{2+}B^{4+}O_3$ system. Our results seem to indicate the existence of a common mechanism of aging.

$(K_{0.99}Li_{0.01})[(Nb_{0.65}Ta_{0.35})_{0.99}Mn_{0.01}]O_3$ ceramics [abbreviated as $(KLi_{0.01})(NbTa_{0.35})O_3-Mn$] were synthesized using a conventional solid-state reaction technique. This compound is based on $KNbO_3$ but modified by adding 35% Ta to the Nb site and 1% Li to the K site. Such modification shifts the tetragonal-orthorhombic phase transition temperature ($T_{t\text{-}o}$) to below room temperature,[4–6] so that the tetragonal phase can persist from room temperature up to T_C. 1% Mn is added to the *B* site, as acceptor dopant. The starting chemicals were K_2CO_3 (99.5%), Li_2CO_3 (99.9%), Nb_2O_5 (99.9%), Ta_2O_5 (99.9%), and MnO_2 (99%). Calcining was done at 950 °C for 2 h in a K_2O-rich atmosphere, and followed by sintering at 1125 °C for 0.5 h in air. Finally, the sintered samples were aged at 80 °C for two weeks. Prior to aging, all the samples were "deaged" by holding at 300 °C for 1 h and were followed by a quick cooling (15 °C/min) to room temperature. The deaged and quenched samples are designated as "unaged" samples. The dielectric permittivity was measured as a function of temperature using HIOKI3532 *LCR* meter with a temperature chamber. The hysteresis loop and electrostrain were measured simultaneously using Radiant Workstation and MTI 2000 photonic sensor. The frequency of the measurement was fixed at 10 Hz.

The dielectric permittivity for the $(KLi_{0.01})\times(NbTa_{0.35})O_3-1Mn$ ceramics as a function of temperature is shown in Fig. 1. Two dielectric peaks are observed at about 164 and 3 °C, respectively. X-ray diffraction characterization indicates that they correspond to the transition temperatures of cubic (paraelectric)-tetragonal (ferroelectric) and tetragonal (ferroelectric)-orthorhombic (ferroelectric), respectively. Therefore, this ceramic has a tetragonal structure throughout the whole temperature range from room temperature up to the T_C (164 °C).

Figure 2 shows a comparison in the hysteresis loop and electrostrain for unaged and aged $(KLi_{0.01})$

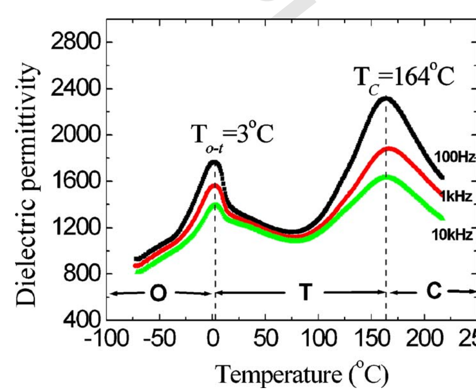

FIG. 1. (Color online) Temperature dependence of dielectric constant of the $(KLi_{0.01})(NbTa_{0.35})O_3-1Mn$ ceramics at the frequencies of 100 Hz, 1 kHz, and 10 kHz. *C*=cubic, *T*=tetrabonal, and *O*=orthorhombic.

[a)]Electronic mail: ren.xiaobing@nims.go.jp

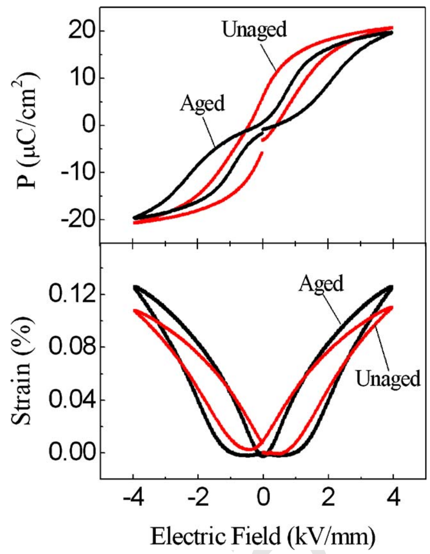

FIG. 2. (Color online) *P-E* hysteresis loop and electrostrain behavior for unaged and aged $(KLi_{0.01})(NbTa_{0.35})O_3-1Mn$ ceramics at room temperature.

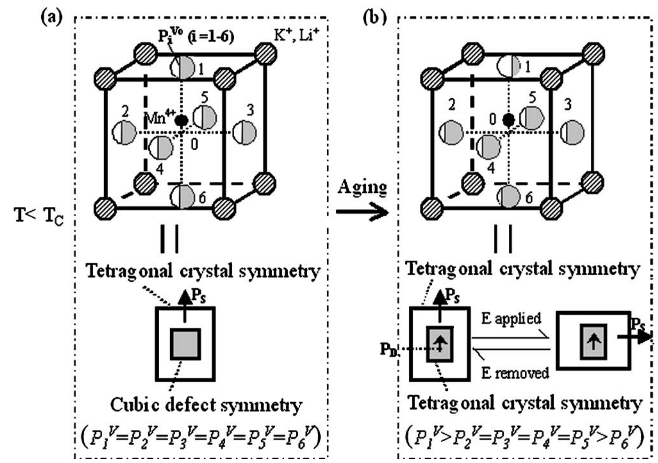

FIG. 3. Defect symmetry and tetragonal crystal symmetry in Mn^{4+}-doped tetragonal $(KLi_{0.01})(NbTa_{0.35})O_3$ structure. (a) unaged (b) aged. $P_i^{V_O}$ is the conditional probability of oxygen vacancy occupying O^{2-} site i ($i=1-6$) next to a given Mn^{4+} (or Mn^{3+}). Large rectangle represents crystal symmetry and small rectangle represents defect symmetry. $\mathbf{P}_S$ refers to spontaneous polarization and $\mathbf{P}_D$ refers to defect polarization.

$\times(NbTa_{0.35})O_3-1Mn$ ceramics at room temperature. In contrast with the normal hysteresis loop for the unaged state, the aged sample shows an interesting double-hysteresis loop, very similar to that of the acceptor-doped $BaTiO_3$-based ceramics after aging.[12,14] We further find that such aging phenomenon also exists in alkaline niobate-based ferroelectrics of different compositions (to be published elsewhere), suggesting that the effect is common in the niobate-based ferroelectrics. Accompanying the double-hysteresis loop, a large recoverable electrostrain of 0.125% at 4 kV/mm is achieved in the aged sample [Fig. 2(b)]. The strain level in the aged sample exceeds that of hard piezoelectric transducer [0.1% at 4 kV/mm (Refs. 15)]. By comparison, the unaged sample shows an irrecoverable strain, which is characterized by the existence of remnant strain when the field restores zero value. It is noted that the remnant strain is not significant for our unaged samples; this is probably due to the constraint effect of the grain boundaries for the polycrystalline samples.

The double-hysteresis loop and the recoverable electrostrain behavior of the aged $(KLi_{0.01})(NbTa_{0.35})O_3-1Mn$ ceramic can be explained by a symmetry-conforming short-range ordering (SC-SRO) mechanism of point defects (i.e., acceptor ions and vacancies), which explained the similar effects in acceptor-doped $A^{2+}B^{4+}O_3$ ferroelectrics[11] and even in ferroelastic martensite.[16,17] Figure 3 presents the symmetry of the statistical distribution of oxygen vacancies around an acceptor ion Mn^{4+} (or Mn^{3+}) in a tetragonal perovskite $A^+B^{5+}O_3$ lattice [$A^+=(K^+,Li^+)$ and $B^{5+}=(Nb^{5+},Ta^{5+})$] for unaged [Fig. 3(a)] and well-aged [Fig. 3(b)] states, respectively. Doping acceptor Mn^{4+}/Mn^{3+} at B^{5+} site necessarily creates oxygen vacancies V_O at O^{2-} sites to keep charge neutrality. We consider Mn^{4+}/Mn^{3+} dopants and O^{2-} vacancies as point defects responsible for the observed aging effect.

For the unaged tetragonal samples, which are formed by immediately cooling down from the cubic paraelectric phase, the SRO distribution of point defects keeps the same cubic symmetry [Fig. 3(a)] as that in the cubic paraelectric phase because the diffusionless paraferroelectric transition cannot alter the original cubic SRO symmetry of point defects.[11] As a result, the unaged ferroelectric state has a tetragonal crystal symmetry, but a cubic defect symmetry; thus the two symmetries are not matching [see the bottom illustration of Fig. 3(a)]. According to the SC-SRO principle,[16,17] such a state is energetically unstable. Therefore, after aging for a long time in the ferroelectric state, defect symmetry gradually changes into a polar tetragonal one, following the polar tetragonal crystal symmetry, as shown in Fig. 3(b). Such a change into polar defect symmetry is realized by the migration of oxygen vacancies during aging, and the polar tetragonal defect symmetry creates a defect polarization $\mathbf{P}_D$, aligning along the spontaneous polarization ($\mathbf{P}_S$) direction [Fig. 3(b)]. When an electric field is applied to the aged tetragonal $(KLi_{0.01})\times(NbTa_{0.35})O_3-1Mn$ sample, $\mathbf{P}_S$ is switched to the field $\mathbf{E}$ direction, but the defect symmetry and associated $\mathbf{P}_D$ cannot have a sudden change, as shown in the bottom illustration of Fig. 3(b). Therefore, after removing the electric field, the unchanged defect symmetry and the associated $\mathbf{P}_D$ cause a reversible domain switching, and consequently a macroscopic double-hysteresis loop and a large recoverable electrostrain behavior, as observed in Fig. 2. Clearly, the explanation is the same as that for acceptor-doped $A^{2+}B^{4+}O_3$ ferroelectrics:[11–14] aging originates from the unmatching of the defect symmetry with the crystal symmetry after a structural transition; it is not sensitive to the structure details such as the valence of the constituent ions. This explains why the aging effect seems insensitive to the valence of the constituent ions in the perovskite structure.

The variation of *P-E* hysteresis loop and electrostrain of the aged sample with temperature is shown in Fig. 4(a). The temperature dependence of the saturation polarization and electrostrain is presented in Fig. 4(b). It can be seen that the aging-induced double-hysteresis loop and recoverable electrostrain behavior can persist up to 140 °C, which indicates a wide temperature range for this effect. However, the maximum polarization and strain gradually decrease with increasing temperature with a gradual drop in recoverability. When temperature exceeds 140 °C, the hysteresis loop becomes a normal one and the strain becomes very small. This may arise from two factors. Firstly, vacancy migration may become so fast at such a temperature that $\mathbf{P}_D$ can follow the change of the electric field direction E. Then $\mathbf{P}_D$ cannot cre-

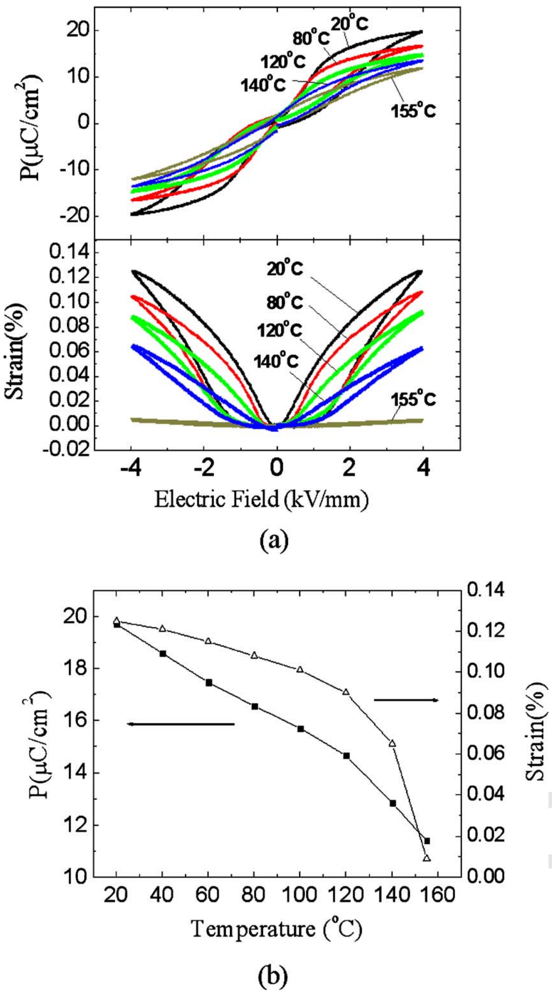

FIG. 4. (Color online) (a) Temperature dependence of *P-E* hysteresis loop and electrostrain of the aged $(KLi_{0.01})(NbTa_{0.35})O_3-1Mn$ ceramics. (b) Temperature dependence of maximum polarization and strain of the aged sample at 4 kV/mm.

ate a restoring force for a reversible domain switching, and the hysteresis becomes a normal one. Secondly, the tetragonality of the ferroelectric phase becomes smaller when close to T_C; this significantly lowers the electrostrain due to domain switching.

We further investigated the stability of the recoverable electrostrain of the aged sample against field cycling. The result is shown in Fig. 5. It shows that the electrostrain has a good recoverability even after 10 000 cycles at 4 kV/mm. Interestingly, the maximum strain increases slightly with increasing number of cycles. This may be due to the migration of a small portion of point defects during the cycling process, which results in a weakening of the defect dipole $\mathbf{P}_D$. As the result, the resistance against domain switching decreases, and hence domain switching becomes easier and more complete. This contributes to a larger strain level.

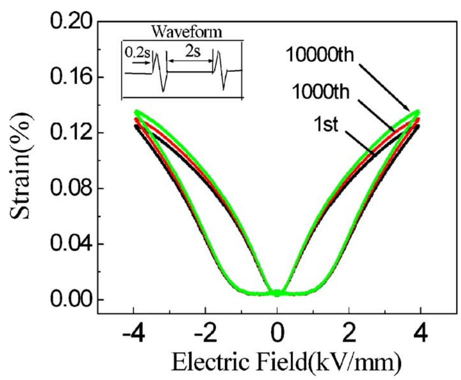

FIG. 5. (Color online) Stability of electrostrain for the aged $(KLi_{0.01})\times(NbTa_{0.35})O_3-1Mn$ ceramics against field cycling. The wave form of the applied field is shown in the inset.

The above results about the aging effect in Mn-doped $KNbO_3$-based ferroelectrics are very similar to those in acceptor-doped $BaTiO_3$ materials.[11–14] The striking similarity in aging behavior between acceptor-doped $A^+B^{5+}O_3$ and acceptor-doped $A^{2+}B^{4+}O_3$ system can be explained by a common mechanism of aging: the symmetry-conforming short-range ordering of point defects. As discussed above, such mechanism relies essentially on symmetry, not on the details of the ionic species. The key idea is that point defects tend to adopt a statistical symmetry that follows the crystal symmetry. This tendency does not depend on the crystal structure or ionic species.[11,16,17]

In conclusion, we found an interesting aging phenomenon, the double-hysteresis loop and recoverable electrostrain behavior, in an acceptor-doped $A^+B^{5+}O_3$ perovskite system: the tetragonal $(KLi_{0.01})(NbTa_{0.35})O_3-1Mn$. The aged sample possesses a large recoverable nonlinear electrostrain of 0.125% at 4 kV/mm. Such effect persists over a temperature range from 20 to 140 °C and shows good stability against field cycling. The aging effect of this $A^+B^{5+}O_3$ compound shows a striking similarity to that of $A^{2+}B^{4+}O_3$ based systems. This similarity suggests a common physical origin of aging. Aging-induced nonlinear electrostrain effect may provide an alternative way to enhance the electromechanical coupling in Pb-free ferroelectric systems. Finally, we note that a slightly pinched hysteresis loop has been reported in a nominally undoped $KNbO_3$-based ferroelectric after thermal cycling.[18] Although no explanation was given, it might bear some relation with the effect we reported here.

This work was supported by Kakenhi of JSPS.

[1]K. Yamanouchi, H. Odagawa, T. Kojima, and T. Matsumura, Electron. Lett. **33**, 193 (1997).
[2]K. Nakamura and Y. Kawamura, IEEE Trans. Ultrason. Ferroelectr. Freq. Control **47**, 750 (2000).
[3]K. Kakimoto, I. Masuda, and H. Ohsato, Jpn. J. Appl. Phys., Part 1 **42**, 6102 (2003).
[4]Y. Saito, H. Takao, T. Tani, T. Nonoyama, K. Takatori, T. Homma, T. Nagaya, and M. Nakamura, Nature (London) **42**, 84 (2004).
[5]M. Matsubara, K. Kikuta, and S. Hirano, J. Appl. Phys. **97**, 114105 (2005).
[6]E. Hollenstein, M. Davis, D. Damjanovic, and N. Setter, Appl. Phys. Lett. **87**, 182905 (2005).
[7]P. V. Lambeek and G. H. Jonker, J. Phys. Chem. Solids **47**, 453 (1986).
[8]W. A. Schulze and K. Ogino, Ferroelectrics **87**, 361 (1988).
[9]U. Robels and G. Arlt, J. Appl. Phys. **73**, 3454 (1993).
[10]K. Uchino, *Ferroelectric Device* (Dekker, New York, 2000), Vol. ■, p. 279. AQ: #1
[11]X. Ren, Nat. Mater. **3**, 91 (2004).
[12]L. X. Zhang, W. Chen, and X. Ren, Appl. Phys. Lett. **85**, 5658 (2004).
[13]L. X. Zhang and X. Ren, Phys. Rev. B **71**, 174108 (2005).
[14]W. F. Liu, W. Chen, L. Yang, L. Zhang, Y. Wang, C. Zhou, S. T. Li, and X. Ren, Appl. Phys. Lett. **89**, 172908 (2006).
[15]S.-E. Park and T. R. Shrout, J. Appl. Phys. **82**, 1804 (1997).
[16]X. Ren and K. Otsuka, Nature (London) **389**, 579 (1997).
[17]X. Ren and K. Otsuka, Phys. Rev. Lett. **85**, 1016 (2000).
[18]J. Zhang, R. Xia, T. R. Shrout, G. Z. Zang, and J. F. Wang, J. Appl. Phys. **100**, 104108 (2006).

AUTHOR QUERIES — 055728APL

#1 Au: Pls. supply vol. no. in Ref. 10